Int. J. Electrochem. Sci., 12 **(2017)** 5628 – 5635, doi: 10.20964/2017.06.94

International Journal of
ELECTROCHEMICAL
SCIENCE
www.electrochemsci.org

Short Communication

Anti-corrosion Performance of Chromium-coated Steel in a Carbon Dioxide-saturated Simulated Oilfield Brine

Yisheng Hu[1*], *Yu Peng*[1], *Feng Hu*[2], *Fangzhou He*[1], *Ping Guo*[1]

[1] State Key Laboratory of Oil and Gas Reservoir Geology and Exploitation, Southwest Petroleum University, Chengdu, 610500, China
[2] Sichuan Geophysical Company, CNPC, Chengdu, 610213, China
[*]E-mail: huyisheng008@yahoo.com

Received: 10 March 2017 / *Accepted:* 28 April 2017 / *Published:* 12 May 2017

A protective chromium coating was prepared on P110 steel by pack cementation. The corrosion behavior of the coated P110 steel in a CO_2-saturated simulated oilfield brine was investigated by static complete immersion tests and electrochemical measurements. The capacitive loop and polarization resistance decreased with increasing immersion time. The temperature of the CO_2-saturated simulated oilfield brine also affected the corrosion behavior. The formation and degradation of the passivation film on the steel were analyzed based on the immersion time and temperature dependence of the electrochemical properties. .

Keywords: Oilfield brine; Corrosion; Electrochemical impedance spectroscopy; Carbon dioxide

1. INTRODUCTION

In the oil industry, N80 carbon steel and low-alloy steel containing 1% chromium (1Cr) are the most widely used construction tubing materials in oil wells [1-3]. Recently, CO_2-enhanced oil recovery (EOR), a well-known and promising oil production method, has received much attention due to its potential in geological carbon storage [4]. Because of the frequent use of EOR and the constant development of deep natural gas reservoirs using CO_2, steel with high CO_2 corrosion resistance is in high demand [5]. Since the development of CO_2-EOR in the 1970's, tubing corrosion by CO_2 has been investigated both experimentally and theoretically [4, 6]. However, engineers still have difficulty designing CO_2-EOR systems in which corrosion can be controlled because of the intrinsic complexity of the process. In oil/gas exploitation, the petroleum tube is a critical structural part of the oil/gas well, accounting for a third of the oil/gas well development costs. Furthermore, 73%-76% of the entire

petroleum tube cost is associated with the oil casing tube [7]. During EOR, the oil casing tubes are subjected to harsh (CO_2-saturated) working conditions, that is, high-pressure, high-temperature and multiphase flow conditions, in the oil/gas well [8]. These tubes directly impact the oil well lifetime, which affects the oilfield lifetime.

Traditionally, surface techniques have been employed to prevent corrosion, abrasion, and oxidation at high temperatures, because these phenomena occur at the surface first [9]. Surface treatments can improve the performance of a material by preventing surface degradation, thus reducing material waste [8, 10-17]. Based on a short-term cost-benefit analysis, using a common carbon steel oil casing tube is economical. Therefore, a steel oil casing tube fabricated from modified steel might be suitable for use in oil/gas production. Thermochemical treatments are a facile, efficient method for synthesizing metallic alloys and protective diffusion coatings on steel that rely on strong metallurgical interactions between the matrix and coating [9, 18-20]. Of the various techniques for preparing diffusion coatings, pack cementation is a cheap and effective method . Accordingly, many processes, such as aluminizing and chromizing, have been performed via pack cementation [21-23]. Although chromizing has been widely used to prevent the abrasion, corrosion and high-temperature oxidation of steel, its application in steel oilfield casing tubes has not attracted public interest [24-27].

Recently, much research has focused on determining the corrosion rate as a function of the Cr content in CO_2 environments. Nevertheless, studies of the Cr content required in low-alloy steel to prevent local corrosion are quite limited, although this information is critical for selecting and using low Cr alloy steel. Xu et al. [2], Kermani and Morshed [3], and Han et al. [4] found that localized corrosion could be eliminated at a Cr content of 3 wt%; however, Chen et al. [28] determined that a Cr content of 4 wt% was necessary to eliminate pitting corrosion. Overall, it was concluded that 1% Cr steel would be locally corroded. This work aimed to modify the structure of 1 wt% Cr steel by adding several alloy elements and heat-treating the material to make it resistant to local corrosion. To achieve this objective, a chromium coating was prepared on the surface of P110 steel by pack cementation. To obtain a better understanding of the corrosion resistance of the chromium coating in a CO_2 environment, the corrosion behavior of the Cr-coated P110 steel in a CO_2-saturated simulated oilfield brine was studied by static complete immersion and potentiodynamic polarization tests. The mass losses, corrosion products and electrochemical corrosion performances of the unmodified and Cr-coated P110 steels were compared to determine the effectiveness of the coating in preventing corrosion.

2. EXPERIMENTS

2.1. Materials

Rectangular (25 mm×20 mm×3 mm) samples were cut from a P110 steel oil casing tube (composition by wt%: C 0.26, Si 0.19, Mn 1.37, P 0.009, S 0.004, Cr 0.148, Ni 0.028, Mo 0.013, Cu 0.019, Nb 0.06, V 0.006, Ti 0.011, Fe balance) using an electrical discharge wire-cutting machine. Then, the samples were ground by hand with SiC abrasive paper, ultrasonically cleaned in an acetone solution, and dried before further treatment.

2.2. Coating fabrication

A pack consisting of 48.5 wt% Al_2O_3, 48.5 wt% Cr, and 3 wt% NH_4Cl was prepared by mixing in a ball mill. The mixing ratio could be obtained from orthogonal tests. The substrate samples and pack compound were placed in an aluminide crucible sealed with a soluble silicate and seat clay mixture and then covered with an aluminide cap. Then, pack cementation was performed in an electric furnace at 100 °C for 8 hours.

2.3. CO_2-saturated simulated oilfield brine preparation

The CO_2-saturated simulated oilfield brine was prepared using analytical reagents and deionized water. The chemical concentrations in the brine were 19 g/L Cl^-, 1.14 g/L SO_4^{2-}, 0.6 g/L HCO_3^-, 0.12 g/L CO_3^{2-}, 11.99 g/L Na^+, 1.05 g/L Mg^{2+} and 0.39 g/L Ca^{2+}. The solution pH was 6.5.

2.4 Weight loss measurement

For the weight loss experiments, the samples were weighed every 5 days using an analytical balance, and the total immersion time was 20 days. During the entire experiment, the solution was refreshed every day to maintain steady-state conditions.

2.5 Electrochemical measurement

For the electrochemical corrosion experiments, an electrochemical measurement system with a three-electrode cell was employed. The reference electrode (RE) and counter electrode (CE) were a saturated calomel electrode (SCE) and platinum sheet, respectively. The working electrode (WE) was a 1 cm^2 clean or coated P110 steel sample. During the EIS experiments, the response was measured every hour after the open circuit potential was stabilized. The frequency range was 10^{-2}-10^5 Hz with a sinusoidal potential perturbation of 1 mV. The EIS data were analyzed using FRA software.

3. RESULTS AND DISCUSSION

Figure 1A shows the EIS data for reinforcing steel samples immersed in the CO_2-saturated simulated oilfield brine for different amounts of time. The Nyquist plots show that the diameter of the capacitive loop remained constant at approximately 120 $k\Omega \cdot cm^2$ when the immersion time was less than 5 days. However, when the immersion time was longer than 10 days, the capacitive loop diameter rapidly decreased. Figure 1B clearly shows that the phase angle decreased as the immersion time was increased to 10 days, and two peaks appeared in the data plot. After immersion for 20 days, the phase angle decreased considerably, indicating that corrosion occurred due to ion penetration [29].

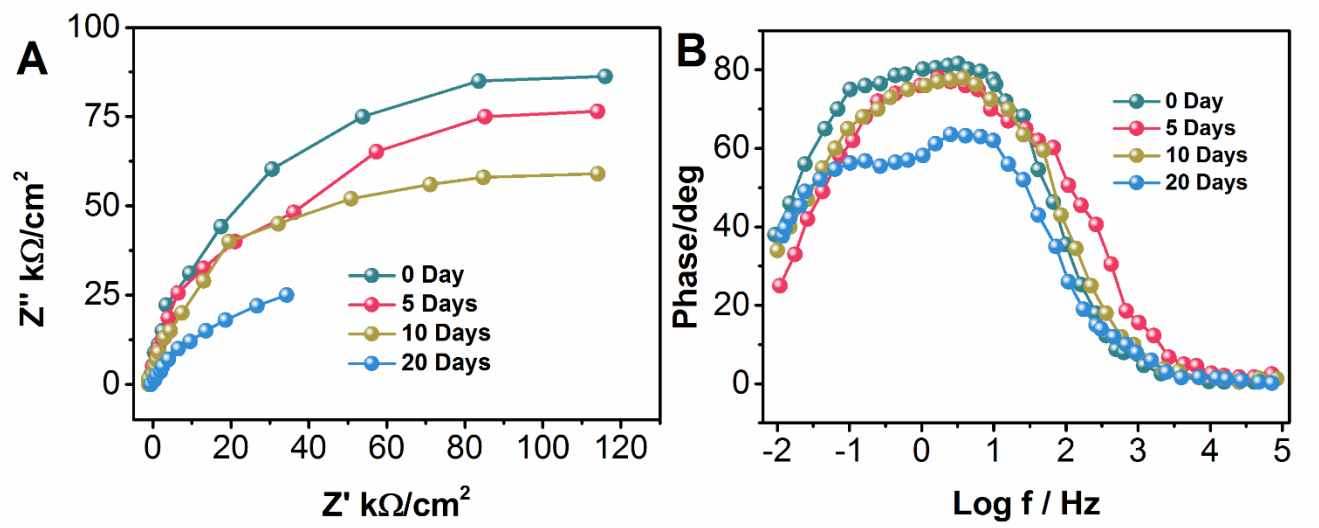

Figure 1. (A) Nyquist and (B) phase angle plots for reinforcing steel samples immersed in the CO_2-saturated simulated oilfield brine for different amounts of time.

Assuming that a passivation film formed on the steel surface and the electrochemical reactions occurred at the metal-film interface, an equivalent circuit could be proposed and fitted to the experimental data [30-32]. Table 1 presents the EIS fitting results for the reinforcing steel. The solution resistance clearly decreased from 75.6 kΩ/cm^2 to 31.5 kΩ/cm^2 with increasing immersion time, due to an increase in its conductivity. The decrease in n_f indicates that as chloride ions permeated the passivation film, it became increasingly non-uniform.

Table 1. EIS fitting results for the reinforcing steel after immersion in the CO_2-saturated simulated oilfield brine for different amounts of time.

Immersion time	R_s (Ωcm^2)	R_f (Ωcm^2)	R_{ct} (Ωcm^2)
0 Day	75.6	144.1	94.5
5 Days	72.4	123.2	89.2
10 Days	53.2	66.2	52.4
20 Days	31.5	0.51	5.22

Figure 2A shows the double layer capacitances (C_{dl}) determined from the data in Table 1. Generally, the capacitance exhibited a positive dependence on the immersion time; it increased dramatically as the immersion time was increased to 10 days and then to 20 days. These results were attributed to the roughening of the sample surface due to pitting corrosion [33]. However, the characteristic C_{dl} value was only in the range of 10-40 μF/cm^2. The relationship between the capacitance C_{dl} and the chloride content is described by the following equation:

$$C_{dl} = \xi_0 \xi A / d$$

where ε and ε_o are the dielectric constants of the medium and the vacuum, respectively; A is the superficial area of the electrode; and d is the double layer thickness of the passivation coating. The capacitance of the steel in the CO_2-saturated simulated oilfield brine increased because (1) the

passivation layer thickness decreased due to its degradation and (2) the electrode surface became increasingly porous due to pitting corrosion by the chloride ions. This latter process increased the surface roughness, which also contributed to the increase in the capacitance. These results demonstrate that the pitting corrosion of the reinforcing steel by the chloride ions in the CO_2-saturated simulated oilfield brine could be monitored by EIS measurements of the capacitance.

Figure 2B shows R_f and R_{ct} as a function of the immersion time. The R_f and R_{ct} values clearly decreased with increasing immersion time, indicating that the passivation layer on the steel surface initially protected it from corrosion. Furthermore, these results imply that the passivation film on the steel surface formed an intact protective coating when the chloride content was below the threshold value [34]. Nevertheless, as the immersion time was increased, the passivation film was gradually destabilized and degraded. At the same time, some pitting pores appeared on the steel surface. Consequently, R_f decreased by an order of magnitude (from 100 to 10 Ω/cm^2) with increasing immersion time.

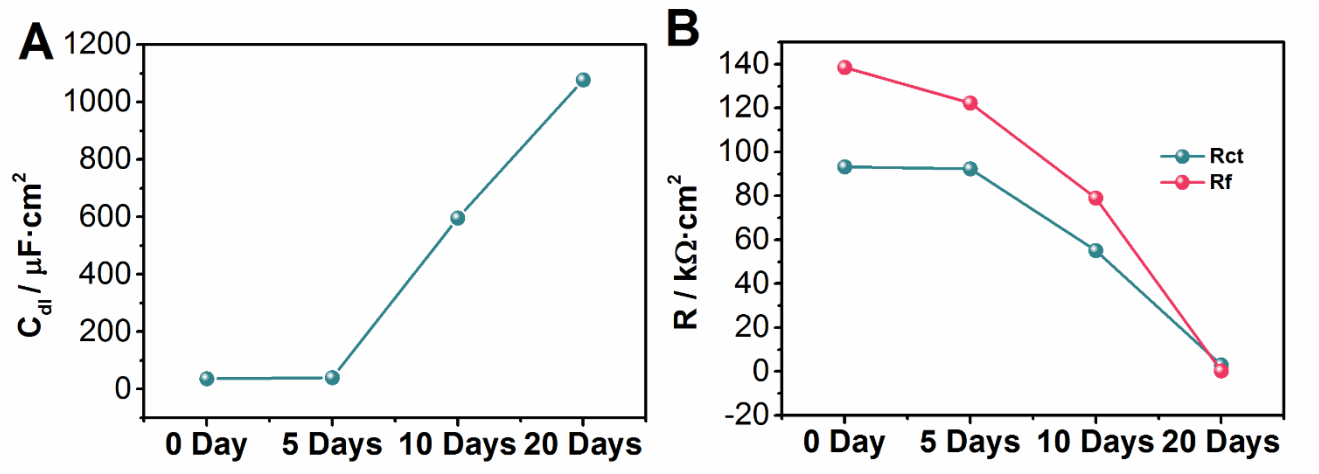

Figure 2. (A) Capacitance and (B) resistance of the reinforcing steel in the CO_2-saturated simulated oilfield brine as a function of the immersion time.

Additionally, Figure 1B shows that the number of peaks in the phase angle data and their magnitudes varied with increasing immersion time. Generally, the number of peaks in the phase angle data corresponded to the number of time constants. Due to the two similar time constants in this system, the peaks overlapped to some degree. For example, at short immersion times, the steel R_f and Y_f values were nearly equal to the R_{ct} and Y_{dl} values, respectively, in the CO_2-saturated simulated oilfield brine. Consequently, the relaxation time constant of the passivation layer was probably comparable to that of the electrochemical reaction, making it difficult to distinguish between them in the phase angle data; only one wide peak was observed in the plot. However, when the immersion time was increased to 10 days, R_{ct} was much higher than R_f due to the depassivation of the passivation film on the sample surface. Accordingly, two peaks appeared in the data plot, and the relaxation and electrochemical reaction time constants could be readily determined. As the immersion time was further increased, the stability of the passivation film gradually decreased, resulting in the observation

of only the relaxation time constant in the data plot. More time constant data for the reinforcing steel in the CO_2-saturated simulated oilfield brine was obtained using Bode plots instead of Nyquist plots.

To analyze the effect of the temperature on the steel corrosion in the CO_2-saturated simulated oilfield brine, EIS measurements were performed for samples immersed at different temperatures for 20 days. Figure 3 shows that the diameter of the Nyquist plot increased with increasing temperature for immersion times shorter than 10 days. At the same time, the phase angle increased, and the corresponding peak broadened. When the immersion time was longer than 10 days, the phase angle peak and capacitive loop diameter decreased slightly. The relaxation time constant of the passivation film was similar to the electrochemical reaction time constant, and therefore, it was difficult to separate them in the Nyquist plots (only a small semicircle was observed) [35, 36].

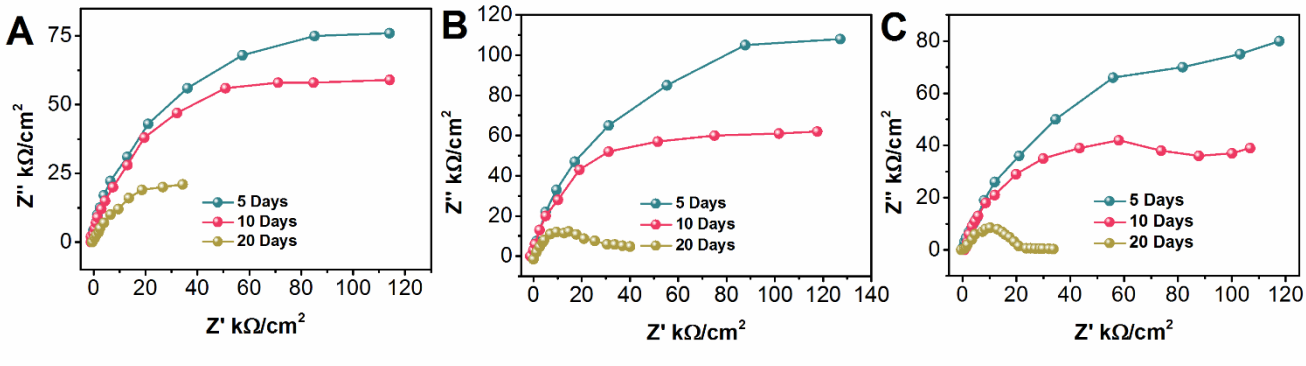

Figure 3. Nyquist plots for the reinforcing steel immersed in the CO_2-saturated simulated oilfield brine at (A) 20 °C, (B) 30 °C and (C) 40 °C.

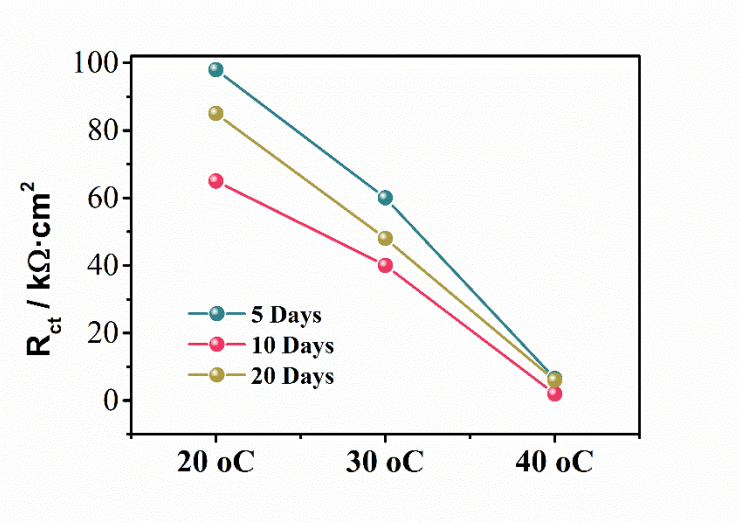

Figure 4. R_f of the reinforcing steel after immersion in the CO_2-saturated simulated oilfield brine for 20 days as a function of temperature.

As shown in Figure 4, the R_f and R_{ct} values were measured to determine the effect of the temperature on the steel corrosion in the CO_2-saturated simulated oilfield brine. At 20 °C, the R_f and

R_{cf} values were higher than 10 kΩ/cm^2 and increased with increasing temperature, indicating that the passivation film thickness increased accordingly. However, when the immersion time was increased to 10 days, these resistances decreased with increasing temperature, due to the depassivation of the passivation film. When the immersion time was 20 days, R_f and R_{cf} decreased significantly to less than 10 kΩ/cm^2, regardless of the temperature.

4. CONCLUSIONS

This work shows that EIS is a promising technique for investigating corrosion in a CO_2-saturated simulated oilfield brine. Generally, the increase in the sample surface roughness due to corrosion was revealed by the increase in the capacitance. The decreases in the resistances (R_f and R_{ct}) to less than 10 kΩ/cm^2 showed that the passivation coating on the reinforcing steel surface was unstable. Furthermore, the coating was locally degraded after immersion in the brine for long periods of time. Finally, the phase angle peaks increased in magnitude and broadened when the steel surface was coated with the passivation film, preventing corrosion.

References

1. S. Zhu, A. Fu, J. Miao, Z. Yin, G. Zhou and J. Wei, *Corrosion Science*, 53 (2011) 3156.
2. S. Guo, L. Xu, L. Zhang, W. Chang and M. Lu, *Corrosion Science*, 63 (2012) 246.
3. M. Kermani and A. Morshed, *Corrosion*, 59 (2003) 659.
4. J. Zhang, Z.L. Wang, Z.M. Wang and X. Han, *Corrosion Science*, 65 (2012) 397.
5. X. Jiang, Y. Zheng, D. Qu and W. Ke, *Corrosion Science*, 48 (2006) 3091.
6. S. Nešić, *Corrosion Science*, 49 (2007) 4308.
7. H. Li, Y. Zhang and L. Han, *Steel Pipe*, 36 (2007) 1.
8. G. Vourlias, N. Pistofidis, D. Chaliampalias, E. Pavlidou, G. Stergioudis, E. Polychroniadis and D. Tsipas, *J. Alloy. Compd.*, 416 (2006) 125.
9. X. Cao, M. Wen and A. Du, Modern metal surface alloying technologies, Chemical Industrial Press, Beijing, 2007.
10. S. Lee, K. Cho, W. Lee and H. Jang, *Journal of Power Sources*, 187 (2009) 318.
11. Z. Wang, J. Lu and K. Lu, *Surface and Coatings Technology*, 201 (2006) 2796.
12. M. Tacikowski, J. Kamiński, J. Rudnicki, T. Borowski, M. Trzaska and T. Wierzchoń, *Vacuum*, 85 (2015) 938.
13. R.V. Lakshmi, G. Yoganandan, A.V.N. Mohan and B.J. Basu, *Surface & Coatings Technology*, 240 (2014) 353.
14. A. Kalendová, D. Veselý, M. Kohl and J. Stejskal, *Progress in Organic Coatings*, 77 (2014) 1465.
15. R. Cottam and M. Brandt, Laser surface treatment to improve the surface corrosion properties of nickel-aluminum bronze, 2015.
16. R.K. Gupta, R. Sundar, B.S. Kumar, P. Ganesh, R. Kaul, K. Ranganathan, K.S. Bindra, V. Kain, S.M. Oak and L.M. Kukreja, *Journal of Materials Engineering and Performance*, 24 (2015) 2569.
17. Y. Matsuzaki, M. Ohya, S. Ajiki, M. Takebe and T. Aso, A Study on Corrosion Rating Process for the Weathering Steel Bridges with Supplemental Rust Cotrolling Surface Treatment, AGU Fall Meeting, 2014, pp. 581.
18. J.M. Kim, T.H. Ha, J.S. Park and H.G. Kim, *Metals - Open Access Metallurgy Journal*, 6 (2016) 29.

19. 19. L.Y. Huang, S.H. Li, H.Q. Zhu, D.Y. Cheng and F.F. Zhang, *Advanced Materials Research*, 1095 (2015) 433.
20. N. Sivanandham, A. Rajadurai, S.M. Shariff, J. Senthilselvan and A. Mahalingam, *Journal of Surface Science & Technology*, 29 (2014) 1.
21. C. Houngninou, S. Chevalier and J. Larpin, *Appl. Surf. Sci.*, 236 (2004) 256.
22. S. Tsipas, H. Omar, F. Perez and D. Tsipas, *Surface and Coatings Technology*, 202 (2008) 3263.
23. X. Peng, C. Xia, Y. Liu and J. Wang, *Surface and Coatings Technology*, 203 (2009) 3306.
24. Y. Zhou, H. Chen, H. Zhang and Y. Wang, *Vacuum*, 82 (2008) 748.
25. Y.-s. HUANG and C.-e. HUANG, *Journal of Shaoguan University (Social Science)*, 6 (2004) 014.
26. Y. An, M. Zhuang, Y. Jie and Z. Li, *Heat Treatment of Metals*, 39 (2014) 68.
27. J. Mondal, J. Kozlova and V. Sammelselg, *Journal of Nanoscience & Nanotechnology*, 15 (2015) 6747.
28. C. Chen, M. Lu, D. Sun, Z. Zhang and W. Chang, *Corrosion*, 61 (2005) 594.
29. Y. Qian, Y. Li, S. Jungwirth, N. Seely, Y. Fang and X. Shi, *Int. J. Electrochem. Sci*, 10 (2015) 10756.
30. A. Carnot, I. Frateur, S. Zanna, B. Tribollet, I. Dubois-Brugger and P. Marcus, *Corrosion Science*, 45 (2003) 2513.
31. A. Hernández-Espejel, M.A. Dominguez-Crespo, R. Cabrera-Sierra, C. Rodríguez-Meneses and E.M. Arce-Estrada, *Corrosion Science*, 52 (2010) 2258.
32. J.-T. Zhang, J.-M. Hu, J.-Q. Zhang and C.-N. Cao, *Progress in Organic Coatings*, 51 (2004) 145.
33. A.K. Singh, G.M. Reddy and K.S. Rao, *Defence Technology*, 11 (2015) 299.
34. L. Yu, R. François, V.H. Dang, V. L'Hostis and R. Gagné, *Cement and Concrete Research*, 67 (2015) 246.
35. Z.S. Asadi and R.E. Melchers, *Reliability Engineering & System Safety*, 162 (2017) 64.
36. C. Cuevas-Arteaga, J.A. Rodriguez, C.M. Clemente, J.M. Rodríguez and Y. Mariaca, *American Journal of Mechanical Engineering*, 2 (2014) 164.